

***In Situ* Imaging of Field-Induced Hexagonal Columns in Magnetite Ferrofluids**

Mark Klokkenburg,<sup>1</sup> Ben H. Erné,<sup>1</sup> Johannes D. Meeldijk,<sup>2</sup> Albrecht Wiedenmann,<sup>3</sup>  
Andrei V. Petukhov,<sup>1</sup> Roel P. A. Dullens,<sup>1</sup> and Albert P. Philipse<sup>1</sup>

<sup>1</sup>Van 't Hoff Laboratory for Physical and Colloid Chemistry, Debye Institute, Utrecht University,  
Padualaan 8, 3584 CH Utrecht, The Netherlands

<sup>2</sup>Electron Microscopy Utrecht, Department of Biology, Utrecht University, Padualaan 8, 3584 CH Utrecht, The Netherlands

<sup>3</sup>Hahn-Meitner-Institut Berlin, Department SF3, Glienickerstrasse 100, D-14109 Berlin, Germany  
(Received 1 August 2006; published 2 November 2006)

Field-induced structures in a ferrofluid with well-defined magnetite nanoparticles with a permanent magnetic dipole moment are analyzed on a single-particle level by *in situ* cryogenic transmission electron microscopy (2D). The field-induced columnar phase locally exhibits hexagonal symmetry and confirms the structures observed in simulations for ferromagnetic dipolar fluids in 2D. The columns are distorted by lens-shaped voids, due to the weak interchain attraction relative to field-directed dipole-dipole attraction. Both dipolar coupling and the dipole concentration determine the dimensions and the spatial arrangement of the columns. Their regular spacing manifests long-range end-pole repulsions that eventually dominate the fluctuation-induced attractions between dipole chains that initiate the columnar transition.

DOI: 10.1103/PhysRevLett.97.185702

PACS numbers: 64.70.Nd, 75.50.Mm, 82.70.Dd

Nanoparticles dispersed in a solvent and with a sufficiently large *permanent* magnetic dipole moment self-assemble into a variety of magnetic equilibrium structures such as (flux-closure) rings and wormlike, branched dipole chains [1,2]. The morphology of these clusters, formed in absence of an external field, has been examined in detail, together with a determination of pair correlation functions and chain-length distributions [3]. In contrast, much less is known about the structural transitions induced by an external (homogeneous) magnetic field for fluids of permanent dipoles. Interestingly, magnetic colloids in an external field are nevertheless frequently encountered in practical applications [4] and biomedicine [5,6].

The structure formation and phase behavior of colloidal systems in reduced dimensions is not necessarily equivalent to that of three-dimensional (3D) systems [7–9]. In particular, for permanent dipolar spheres confined to two dimensions (2D) a field-induced transition to a columnar phase with local hexagonal symmetry was predicted [10], although a conclusive experimental real-space analysis is still lacking. Elongated iron-particle clusters have been imaged [1] but the irregular particle shape and the bidisperse size distribution obstruct the wanted single-particle analysis. Parallel structures have also been observed for maghemite ferrofluids dried in the presence of a homogeneous field [11,12]. However, we have shown elsewhere that drying procedures may drastically change structure morphology [2]. Moreover, dipole interactions in conventional ferrofluids are in general too weak for a realistic comparison to the purely dipolar spheres from simulations.

In this Letter, we report unequivocal real-space evidence for the predicted columnar phase transition [10] from *in situ* cryo-TEM images of monodisperse magnetic colloids with dominating dipolar interactions. The particle positions are confined by a 2D film whereas the dipole

orientations can thermally fluctuate in 3D. Our imaging results, in addition, allow to quantify positional and angular interparticle correlations showing, among other things, a progressive distortion of the local hexagonal symmetry for decreasing particle dipole moments.

The permanently magnetic particles in this study are monodisperse magnetite ( $\text{Fe}_3\text{O}_4$ ) colloids with a surfactant shell such that the pair interaction comprises only a steep contact repulsion and a dipolar potential  $x/r^3$ , where  $x$  is the angular dependent amplitude of two dipoles at a center-to-center distance  $r$ . The maximal dipolar attraction for two dipoles in head-to-tail configuration is  $V_{\max} = -\mu_0\mu^2/(2\pi k_B T d^3)$ , where  $\mu_0 = 4\pi \times 10^{-7} \text{ J A}^{-2} \text{ m}^{-1}$ ,  $\mu$  is the magnetic dipole moment of one particle,  $k_B$  is the Boltzmann constant,  $T$  the absolute temperature, and  $d$  the hard core diameter, including the surfactant shell. The interaction of the dipoles with the applied magnetic field is  $\epsilon = -\mu\mu_0 H/(k_B T)$ , where  $H$  is the external magnetic field strength.

Two colloidal magnetite dispersions (*A* and *B*) in Decalin were prepared following [2]. The average particle diameter ( $d$ ) according to TEM (including the 2 nm surfactant layer), the values for the dipolar contact attraction  $V_{\max}$ , and the interaction of the particles with the magnetic field  $\epsilon$  are listed in Table I. Cryo-TEM images of vitrified dispersion films (thickness of  $1d$ ) prepared in a homogeneous magnetic field (0.2 T) were obtained for systems *A* and *B*. To track particle positions in 2D snapshots, we used image analysis software [13].

The arrangement of the dipolar particles in an external field (Fig. 2) is for both systems markedly different from the structure formation in zero field (Fig. 1) [3]. In system *A*, where the dipole-dipole attractions do not exceed  $4k_B T$ , relatively long ( $>60d$ ), but rather diffuse sheets are formed of loosely bound chains with a width in the range 1–10 $d$ ,

TABLE I. Sample characteristics of systems *A* and *B*.

Code	<i>A</i>	<i>B</i>
$d_{\text{TEM}}$ (nm)	$20.1 \pm 2.6$	$24.0 \pm 2.4$
Dipole-dipole attraction $V_{\max}$ ( $k_B T$ ) <sup>a</sup>	-4	-9
Interaction ( $\epsilon$ ) with 0.2 T at 300 K ( $k_B T$ )	-32	-76

<sup>a</sup>Determined using the dipole moment of the particles directly obtained from magnetization curves and the interparticle distance obtained from radial distribution [ $g(r)$ ] analysis of cryo-TEM data.

separated by a typical average distance of about 260 nm ( $13d$ ). A clear structural transition from loosely bound chains to tightly packed long ( $>80d$ ) columns is observed when  $V_{\max}$  is increased to -9 (system *B*). Because of the strong dipole-dipole interaction and the strong coupling to the magnetic field ( $\epsilon = -76$ ) linear dipolar chains are formed that join into uniform columns with hexagonal order and a limited number of lens-shaped voids [see Fig. 2(b)1 and 2(b)2, open circles]. These voids likely are kinetically arrested defects whose relaxation requires simultaneous displacement of many neighboring dipoles. Furthermore, the columns all have a similar width of about  $5d$  and are equally spaced with a characteristic distance of 330 nm ( $14d$ ), manifesting a significant long-range repulsion between the stiff elongated sheets. Upon lowering the particle concentration by a factor of 4, the columns laterally shrink to strands of about two dipole chains [see inset Fig. 2(b)1]. The observations validate the simulation results of quasi-2D dipolar hard-sphere systems at comparable interactions by Satoh *et al.* [14] and by Weis [10], the latter also showing a columnar phase that exhibits hexagonal symmetry and a column spacing of order  $10d$ .

Within the columns, two neighboring chains are generally shifted by  $(1/2)d$ , which is energetically favorable [15]. For rigid aligned chains that are out of registry, the lateral chain-chain interaction scales with the dipole-dipole attraction and with the length of the chains [16]. In system *A*, the short-range attraction between the chains is clearly much weaker than in system *B*.

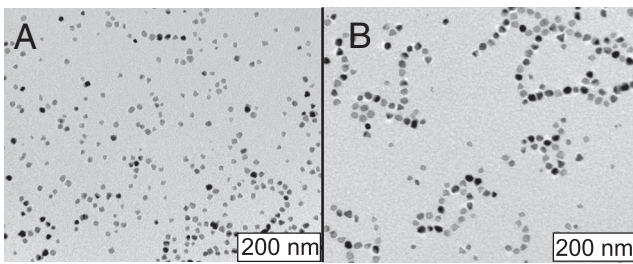


FIG. 1. Typical *in situ* cryo-TEM images of vitrified magnetite dispersions *A* and *B* in zero field. The surface fraction for both systems is 0.14 [3]. In a homogeneous field a transition occurs to equal-spaced columns as shown in Fig. 2.

Thermal fluctuations [15], defective chains [17], or chain bending in general [18] can induce variations in the dipole moment density and, consequently, long-range coupling between one-dimensional structures in colloidal dispersions. In system *A*, fluctuations in the dipole moment density must be important, particularly in view of the initial particle configuration in zero field (Fig. 1), which consists of deflective chains. As the relatively short dipolar chains in zero field easily form and break up, the induced attractions are limited. Consequently, the observed columns are rather diffuse and have a liquidlike structure, in contrast to the *B* system.

For the columns to grow in system *B*, they have to adsorb neighboring chains. However, as this process advances, the columns become more rigid such that fluctuation attractions vanish. Instead, the end poles of the rigid magnetic columns cause neighboring columns to repel one another, leading to the observed regular spacing between the columnar aggregates, which resemble the structures observed in MR fluids [19].

To show that these systems are indeed quasi-2D, the field was rotated by  $90^\circ$  and applied perpendicular to the film of magnetite dispersion *B* prior to vitrifying it. Consequently, up to  $4.5k_B T$  of repulsion is introduced and almost all clusters break apart, leading to a gaslike configuration of single particles [inset of Fig. 2(b)2]. This configuration also confirms that dipolar attractions dominate the column formation in our fluids since no isotropic clusters are observed.

To quantify the internal column structure, the coordination number probability was calculated, defining a neighbor as being located within a center-to-center distance of  $r_c = 1.35d$  [Fig. 3(a)]. The distribution shows a broad band for the *A* particles, whereas it clearly peaks at 4 and 6 in system *B*, corresponding to, respectively, outer and inner chains in a column. For comparison, for zero-field dipolar structures the most probable coordination number is 2 [3], confirming the self-assembly of particles in single linear chains (see Fig. 1). The difference between structures is even more pronounced in the nearest neighbor angle distribution in Fig. 3(b), which quantifies the local orientational order in the columns. For small interactions, only moderate orientational correlation is observed in the  $0^\circ$  (parallel to the magnetic field) and the  $180^\circ$  (antiparallel to the magnetic field) directions, manifesting the presence of uncorrelated linear chains. The orientational order is drastically enhanced in system *B*, where peaks are observed at multiples of  $60^\circ$ , manifesting a hexagonal particle configuration. Because of the local fluctuations, the peaks are considerably broad.

To better highlight the differences in the orientational order at the particle length scale, we computed the local bond-orientational order parameter  $\psi_6$  [9]:

$$\psi_6(r_i) = \frac{1}{N} \sum_{j=1}^N \exp[6i\theta(r_{ij})], \quad (1)$$

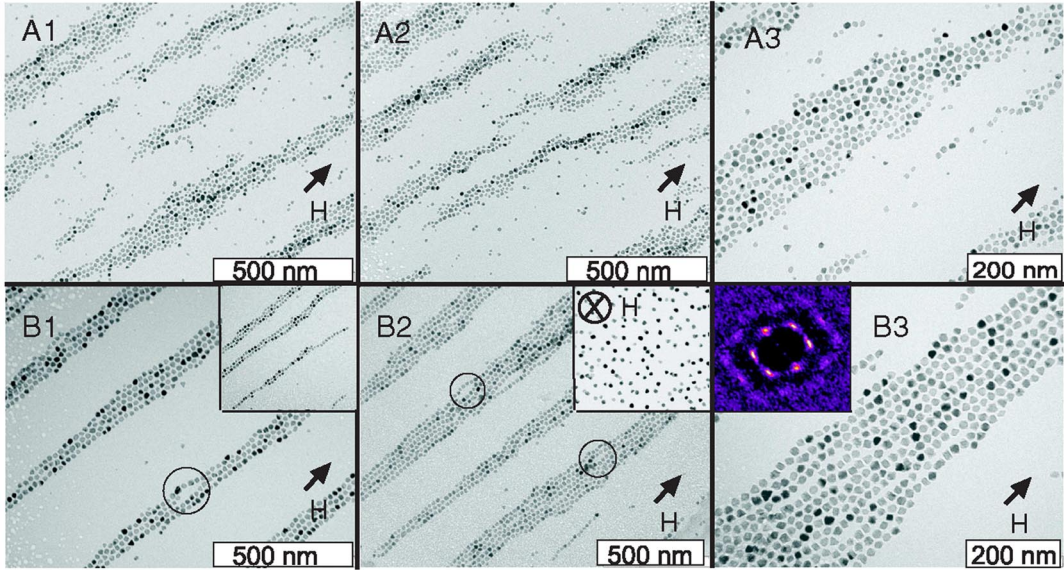


FIG. 2 (color online). Typical *in situ* cryo-TEM images of magnetite dispersion *A* [(A1)–(A3)] and *B* [(B1)–(B3)], vitrified in the presence of an in-plane homogeneous magnetic field (0.2 T). The surface fraction  $\theta$  is 0.25 for both systems. Open circles mark the imaged lens-shaped voids in the magnetic sheets. The inset in panel (B1) shows the structures upon dilution by a factor 4. The inset in panel (B2) demonstrates that orienting the field perpendicular to the film melts columns to a gas of repulsive dipoles. The inset in panel (B3) is the 2D structure factor [ $S(q)$ ] calculated for the cryo-TEM images.

where the summation  $j$  runs over the total number of nearest neighbors  $N$  of a particle  $i$ .  $\theta(r_{ij})$  is the angle between the bond vector connecting particles  $i$  and  $j$  and an arbitrary fixed reference axis. Averaging over all par-

ticles  $i$  yields the average hexagonal order parameter  $\langle|\psi_6|\rangle$ , which is approximately 0.4 for a fluid and 1 for a perfect 2D hexagonal crystal. In systems *A* and *B*,  $\langle|\psi_6|\rangle$  values of 0.49 and 0.57 were obtained, respectively, indicating a significant but not dramatic increase in hexagonal order with growing dipolar attractions. To visualize these results, the  $\psi_6$  values of the particles in Fig. 2(a)3 and 2(b)3 are displayed in Fig. 4 using color codes. Note that the number of particles with  $\psi_6 \geq 0.8$  is the highest for system *B* and that these particles are more frequently each other's neighbors, confirming significant differences in both the local orientational order and the correlation lengths of the particles in systems *A* and *B*.

Information on the translational correlation lengths is obtained by calculating the radial distribution function  $g(r)$

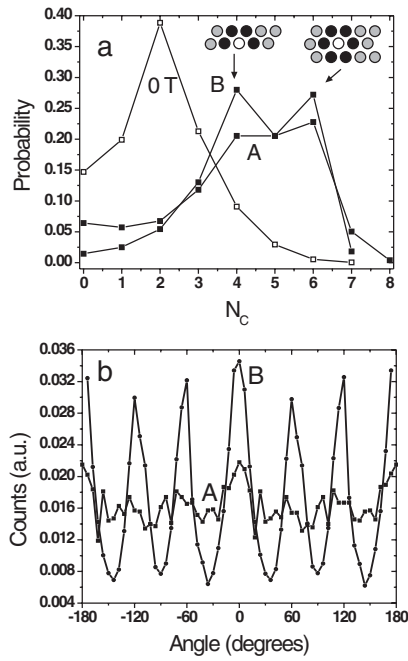


FIG. 3. (a) Histogram of the coordination number  $N_c$  probability of a particle in ferrofluid *A* and *B*. The open symbols correspond to the probability observed in zero field (0 T) [3]. (b) Nearest neighbor angle distributions for the *A* particles and the *B* particles.

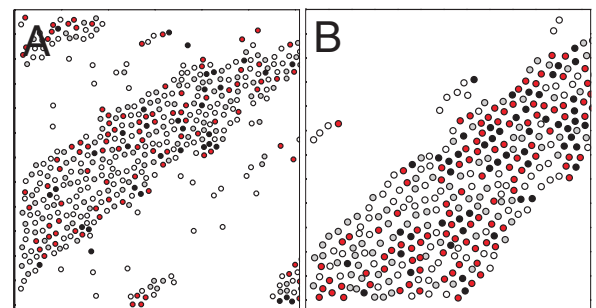


FIG. 4 (color online). Bond-orientational order parameter  $\psi_6$  values for the individual particles in the corresponding images Fig. 2(a)3 (A) and Fig. 2(b)3 (B). The color code for the  $\psi_6$  values is as follows:  $1.0 \geq \psi_6 \geq 0.8$  (black),  $0.8 > \psi_6 \geq 0.6$  (red),  $0.6 > \psi_6 \geq 0.4$  (gray), and  $\psi_6 < 0.4$  (white).

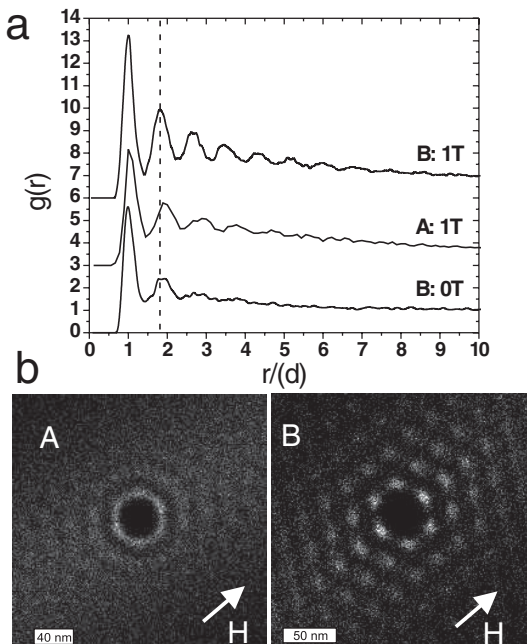


FIG. 5. (a) Radial distribution function  $g(r)$ . The curves have been shifted vertically for clarity. The dotted line corresponds to the peak positions observed in zero field [3]. (b) Two-dimensional correlation function.

[Fig. 5(a)]. For strong interactions ( $V_{\max} = -9$ ), the data show peaks that manifest correlations extending over more than 6 particles diameters. In contrast, data obtained recently in zero field show only clear correlations up to 2 particle diameters [3]. The hexagonal arrangement of the particles leads to a shift of the second peak in  $g(r)$  to  $\sqrt{3}d$ . To examine more precisely the hexagonal conformation of the particles, the two-dimensional correlation function  $g(x, y)$  is more appropriate. As demonstrated in Fig. 5(b), there is no clear translational correlation in any distinct direction in system A, since only a diffuse ring is observed at  $1d$  and  $2d$ , leading to the first two peaks in the radial distribution function  $g(r)$ . However, in system B a distorted hexagonal correlation pattern is observed with the first peaks at  $1.0d$  (parallel to the field) and at  $1.1d$  (perpendicular to the field), indicating that the interparticle distance is 10% longer perpendicular to the magnetic field, due to fluctuations in the distance between the parallel chains. A Fourier transform of the field-induced columns [inset of Fig. 2(b)] corroborates the elongated hexagonal symmetry. Strong similarities are found with neutron scattering patterns obtained on cobalt ferrofluids in 3D [20]. Our results therefore suggest that formation of 2D columns also occurs in 3D systems.

In summary, we have demonstrated that sterically stabilized nanoparticles with a sufficiently large permanent magnetic dipole moment form columns with distorted

hexagonal symmetry in the presence of an in-plane magnetic field, confirming the existence of the structures predicted by 2D simulations of dipolar hard spheres. A quantitative analysis shows a progressive distortion of the local hexagonal symmetry for decreasing particle dipole moments. The regular spacing between the columns shows that their nucleation and growth is an interplay between short-range attraction between single dipolar chains and long-range repulsion between the end-poles of the columns.

Willem Kegel is thanked for useful discussions. Volkert de Villeneuve is thanked for his help with the data analysis.

- [1] K. Butter, P. H. H. Bomans, P. M. Frederik, G. J. Vroege, and A. P. Philipse, *Nat. Mater.* **2**, 88 (2003).
- [2] M. Klokkenburg, C. Vonk, E. M. Claesson, J. D. Meeldijk, B. H. Erné, and A. P. Philipse, *J. Am. Chem. Soc.* **126**, 16 706 (2004).
- [3] M. Klokkenburg, R.P.A. Dullens, W.K. Kegel, B.H. Erné, and A.P. Philipse, *Phys. Rev. Lett.* **96**, 037203 (2006).
- [4] K. Raj and R. Moskowitz, *J. Magn. Magn. Mater.* **85**, 233 (1990).
- [5] A. S. Lubbe, C. Alexiou, and C. Bergemann, *J. Surg. Res.* **95**, 200 (2001).
- [6] Q. A. Pankhurst, J. Connolly, S. K. Jones, and J. Dobson, *J. Phys. D: Appl. Phys.* **36**, R167 (2003).
- [7] S. Neser, C. Bechinger, P. Leiderer, and T. Palberg, *Phys. Rev. Lett.* **79**, 2348 (1997).
- [8] F. Ramiro-Manzano, F. Meseguer, E. Bonet, and I. Rodriguez, *Phys. Rev. Lett.* **97**, 028304 (2006).
- [9] D. R. Nelson, *Defects and Geometry in Condensed Matter Physics* (Cambridge University Press, Cambridge, England, 2002), pp. 68–91.
- [10] J.J. Weis, *Mol. Phys.* **103**, 7 (2005).
- [11] L. N. Donselaar, P. M. Frederik, P. Bomans, P. A. Buining, B. M. Humbel, and A. P. Philipse, *J. Magn. Magn. Mater.* **201**, 58 (1999).
- [12] Y. Lalatonne, J. Richardi, and M. P. Pilani, *Nat. Mater.* **3**, 121 (2004).
- [13] J. C. Crocker and D. G. Grier, *J. Colloid Interface Sci.* **179**, 298 (1996).
- [14] A. Satoh, R. W. Chantrell, S. I. Kamiyama, and G. N. Coverdale, *J. Colloid Interface Sci.* **178**, 620 (1996).
- [15] T.C. Halsey and W. Toor, *Phys. Rev. Lett.* **65**, 2820 (1990).
- [16] E. M. Furst and A. P. Gast, *Phys. Rev. E* **62**, 6916 (2000).
- [17] J. E. Martin, K. M. Hill, and C. P. Tigges, *Phys. Rev. E* **59**, 5676 (1999).
- [18] M. Gross and S. Kiskamp, *Phys. Rev. Lett.* **79**, 2566 (1997).
- [19] M. Ivey, J. Liu, Y. Zhu, and S. Cutillas, *Phys. Rev. E* **63**, 011403 (2000).
- [20] A. Wiedenmann, A. Hoell, M. Kammler, and P. Boesecke, *Phys. Rev. E* **68**, 031203 (2003).